IEEE Access
Multidisciplinary | Rapid Review | Open Access Journal

Received November 19, 2018, accepted December 6, 2018, date of publication December 11, 2018,
date of current version January 23, 2019.

Digital Object Identifier 10.1109/ACCESS.2018.2886222

An Adaptive Terminal Sliding Mode Control for Robot Manipulators With Non-Singular Terminal Sliding Surface Variables

ANH TUAN VO AND HEE-JUN KANG
School of Electrical Engineering, University of Ulsan, Ulsan 44610, South Korea

Corresponding author: Hee-Jun Kang (hjkang@ulsan.ac.kr)

This research was supported by Basic Science Research Program through the National Research Foundation of Korea (NRF) funded by the Ministry of Education (NRF-2016R1D1A3B03930496).

ABSTRACT This paper presents an adaptive terminal sliding mode control (TSMC) algorithm for robot manipulators. The contribution of our control method is that the suggested controller can enable the advantages of non-singular TSMC such as non-singularity, high robustness, small transient error, and finite time convergence. To develop the suggested system, a non-singular terminal sliding variable is selected and does not have any complex-value or constraints of the exponent in conventional TSMC. Therefore, it prevents the singularity that occurs in the conventional TSMC and eliminates the reaching phase glitch. Accordingly, the suggested system can ensure that the controlled variables reach the desired values within a randomly known finite time using an efficiently smooth and chattering-free definite control input. In addition, sliding motion in finite time can be achieved by employing the adaptive self-tuning rules with no prior information regarding the upper bounds of undefined parameters (e.g., friction, disturbances, and uncertainties). Furthermore, the finite-time convergence and global stability of the proposed algorithm are proved by the Lyapunov stability theory. Finally, the proposed control algorithm is applied to the joint position tracking control simulation for a 3-DOF PUMA560 robot. The trajectory tracking performance of the proposed method is compared with those of the conventional terminal sliding mode control and the conventional continuous sliding mode control. This comparison shows the efficiency and superiority of the proposed algorithm.

INDEX TERMS Non-singular terminal sliding mode control, robotic manipulator, adaptive self-tuning rules, uncertainty, disturbance, chattering behavior.

I. INTRODUCTION

During recent decades, considerable research efforts have been devoted to investigating robot manipulator control systems. To achieve higher-precision tracking performance, numerous control methods have been constructed for motion control of robot manipulators, such as the proportional-integral-derivative (PID) controller [1] and computed torque controller (CTC) [2]. Those mentioned controllers were highlighted as simple and monotonic methods for robot control. Generally, dynamic models of robot manipulators have been challenged with various parametric uncertainties consisting of friction, perturbation, payload parameters, and sensor noise. Unfortunately, those controllers do not exhibit good control performance of highly nonlinear and uncertain control systems. Accordingly, to handle the uncertainty of robotic systems and to improve the control performance, recently, many nonlinear methods have been suggested for robot manipulators such as adaptive control [3], [4], fuzzy control [5], [6], optimal control [7], neural network control [8], [6], and sliding mode control [9]–[12].

Sliding mode control (SMC) has been a useful and impressive robust control methodology to correct deficiency from any kind of uncertainties or perturbation for both linear and nonlinear systems. The scheme of SMC is to firstly perform a sliding manifold and then build up a control principle that obligates the controlled variables to attain and maintain the sliding surface. Nonetheless, in real systems, the primary weakness of SMC is an undesirable chattering behavior caused by high-frequency switching. Furthermore, this algorithm only stabilizes the system asymptotically in

the sliding phase following a linear sliding manifold methodology. From this point of view, the controlled variables cannot obtain the desired values within a finite amount of time.

In 1990s, a new category of SMC called terminal sliding mode control (TSMC) was originally published by Venkataraman and Gulati [13] and then advanced by Zhihong *et al.* [14] and Wu *et al.* [15]. Contrary to linear sliding surfaces, nonlinear sliding hyperplanes have exposed some advanced properties in terms of high robustness, fast transient response, high tracking positional accuracy, and finite time convergence. Therefore, various uses of the TSMC method have been established (e.g., robot control [14], [16], motor control [17], TSMC observer [18].) Nonetheless, this control algorithm does not exhibit good convergence when the controlled variables are distant from the desired values. Specifically, the TSMC algorithm has encountered the singularity drawback that causes complex-value, exponent, and a greater control effort. To increase convergence speed once the controlled variables are significantly different from the desired values, Yu and Zhihong [19] and Yang and Yang [20] presented a fast terminal sliding mode control (FTSMC). However, both of the above methods still encounter the singularity drawback. So, to deal with this obstacle, several non-singular TSM (NTSM) methods [20]–[22] based on TSMC have been established.

In addition, those above-mentioned control algorithms require information regarding the upper bound of the uncertainties in the robot system, eliminating them from control input signals. In general, it is not easy to precisely define the upper bound of the uncertainty. Some control methods, which are based on an integration of adaptive control law, fuzzy logic control, neural network control, or synchronization control into TSMC or NTSMC to overcome above issue, have been presented ([23]–[33] and reference therein). In those papers, adaptive laws were used only to determine unidentified parameters. These methods still required information on the upper bound of the unidentified parameters, but no attention was paid to disturbances and uncertainties. Other approaches [19]–[22] utilized TSM manifolds, but also encountered the singularity drawback. To prove convergence in finite time, those algorithms ordered the approximately large estimated parameters to generate initial values. However, such techniques are not practically possible since the magnitude of the generated control input seems to be not suitable in terms of motor torque saturation during the period of manifold switching, $s = 0$ and $s \neq 0$. Another critical problem is that a chattering phenomenon occurred by applying high-frequency control switching, which reduces the tracking control performance. Some procedures have also used a *sat* $(\cdot)$ function, sometimes called a relay function, but those techniques reduce tracking positional accuracy and increase steady-state errors. So, the robustness and performance of the control algorithm will be degraded.

Purposed by the above analysis, the target of our paper is to propose a novel tracking control algorithm for robot manipulators. The benefits of our control methodology are highlighted as:

- Satisfies updating rules to control the system's controlled variables, attains the sliding manifold, and converges to the balanced point in finite time, as well as guarantees asymptotic stability of the robot system with a fast transient response rate.
- Not only prevents the singularity problem by presenting a modified NTSM surface, but also avoids the reaching phase issue.
- Eliminates the requirement for prior information about the upper bounds of parametric uncertainties existing in a real robotic system.
- Rejects the effect of chattering behavior in control input.
- Finite time convergence characteristic and asymptotic stability of the robot system are proved by the Lyapunov criterion.

The rest of our article is arranged as follows. The problem statements required for the proposed non-singular sliding surface and control are presented in Section 2. The structural procedure of the suggested control algorithm is reported in Section 3. In Section 4, the proposed control algorithm is applied to the joint position tracking control simulation for a 3-DOF PUMA560 robot. Further, the proposed algorithm's trajectory tracking performance is compared with those of the conventional TSMC and conventional sliding mode control. Lastly, several concluding remarks are presented in Section 5.

Several symbols are utilized throughout the article, $\|*\|$ and $|*|$ correspond to the Euclidean norm and modulus, while $\mathbb{N}$ and $\mathbb{R}$ correspond to the spaces of natural numbers and real numbers, respectively.

II. PROBLEM STATEMENT

For an n-link rigid robotic manipulator, the corresponding dynamic equation can be given as ([22])

$$M(\theta)\ddot{\theta} + C_m\left(\theta, \dot{\theta}\right)\dot{\theta} + G(\theta) + F_r\left(\dot{\theta}\right) + \tau_D = \tau \quad (1)$$

in which $\theta, \dot{\theta}, \ddot{\theta} \in \mathbb{R}^n$ are defined as the system's state vector. $M(\theta) \in \mathbb{R}^{n\times n}$ is the inertia matrix, $C_m\left(\theta, \dot{\theta}\right) \in \mathbb{R}^{n\times 1}$ is defined as the matrix resulting from Coriolis and centrifugal forces, $G(\theta) \in \mathbb{R}^{n\times 1}$ is the gravitational force term, $F_r\left(\dot{\theta}\right) \in \mathbb{R}^{n\times 1}$ is the friction matrix, $\tau \in \mathbb{R}^{n\times 1}$ is the torque produced by actuators, and $\tau_D \in \mathbb{R}^{n\times 1}$ is a load disturbance matrix.

From Eq. (1), we have

$$\ddot{\theta} = M^{-1}(\theta)\left[\tau - C_m\left(\theta, \dot{\theta}\right)\dot{\theta} - F_r\left(\dot{\theta}\right) - G(\theta) - \tau_D\right] \quad (2)$$

To simplify the analysis and design in next section, Eq. (2) can be given as

$$\ddot{\theta} = H\left(\theta, \dot{\theta}\right) + D\left(\theta, \dot{\theta}, t\right) + Q(\theta)\tau \quad (3)$$

in which $H\left(\theta, \dot{\theta}\right) = M^{-1}(\theta)\left[-C_m\left(\theta, \dot{\theta}\right)\dot{\theta} - G(\theta)\right]$, $Q(\theta) = M^{-1}(\theta)$, and $D\left(\theta, \dot{\theta}, t\right) = M^{-1}(\theta)\left[-F_r\left(\dot{\theta}\right) - \tau_D\right]$. Next, we employ $u(t) = \tau$ as the control input and $\mathrm{x} = [x_1, x_2]^T$ as the state vector in which x_1, x_2 correspond

to $\theta, \dot{\theta} \in \mathbb{R}^{n\times 1}$. The robotic dynamic of Eq. (3) can be described in the following state space form as

$$\begin{cases} \dot{x}_1 = x_2 \\ \dot{x}_2 = H(\mathrm{x}, t) + D(\mathrm{x}, t) + Q(\mathrm{x}, t)\, u(t) \end{cases} \tag{4}$$

in which $H(\mathrm{x}, t) \in \mathbb{R}^n$ and $Q(\mathrm{x}, t) \in \mathbb{R}^{n\times n}$ are smooth nonlinear vector fields, and $D(\mathrm{x}, t) \in \mathbb{R}^n$ presents the disturbances and uncertainties.

The sliding motion in finite time can occur with no prior information regarding the upper bounds of undefined parameters (e.g., friction, disturbances, and uncertainties), and the following assumption is necessary for designing a control scheme in the next section.

Assumption 1: There exists a bounded function of $D(\mathrm{x}, t)$ presenting undefined parameters (e.g., friction, disturbances, and uncertainties), which satisfies the following condition:

$$D(\mathrm{x}, t) \leq \Psi \tag{5}$$

The control target in our article is to construct a suggested control algorithm such that the system's controlled variables of x_1 attain the desired values of x_d within a finite amount of time with no prior information about upper bounds of undefined parameters. Accordingly, the tracking positional error is defined as follows:

$$e = x_1 - x_d \tag{6}$$

To achieve this target, this paper presents two main tasks: (1) construct apposite NTSM manifolds including the desirable dynamic features and (2) establish a control algorithm to guarantee the sliding movement and the system's controlled variables to achieve the desired trajectory within a finite time.

III. DESIGN PROCEDURE OF THE CONTROL ALGORITHM

In this section, a novel control algorithm is proposed for the robot manipulator of Eq. (1) and is expressed by following two main tasks.

A. DESIGN OF THE NON-SINGULAR TERMINAL SLIDING MODE SURFACE

First, with the tracking error in Eq. (6), the following NTSM surface variables are suggested:

$$s = \dot{e} + \int_0^t \left(g_0 e^{[\gamma]} + g_1 e + g_2 e^3 + g_3 \dot{e}^{[\beta]} \right) \tag{7}$$

in which $s = [s_1, s_2, \ldots, s_n]^T \in \mathbb{R}^{n\times 1}$ is the sliding variable; g_0, g_1, g_2, g_3 are positive coefficients; $0 < \gamma < 1$, $\beta = 2\gamma / (1+\gamma)$, and $e = [e_1, e_2, \ldots, e_n]^T \in \mathbb{R}^{n\times 1}$ are tracking errors; and $\dot{e} = [\dot{e}_1, \dot{e}_2, \ldots, \dot{e}_n]^T \in \mathbb{R}^{n\times 1}$ is the time derivative of the tracking error of e.

In addition, $e^{[\gamma]}$ and $\dot{e}^{[\beta]}$ are defined as ([34])

$$e^{[\gamma]} = |e|^{\gamma} sign[e] \text{ and } \frac{d}{dt} e^{[\beta]} = \beta |e|^{\beta-1} \dot{e} \tag{8}$$

in which $\gamma > 0$, $\beta > 0$, and $sign[e] = \begin{cases} 1 \text{ if } e > 0 \\ -1 \text{ if } e < 0 \\ 0 \text{ if } e = 0 \end{cases}$

Remark 1: The converging speed property of the NTSM variable has been explained in [20]. Once the tracking positional error of $|e|$ is much greater than 1, $g_0 e^{[\gamma]} + g_1 e + g_2 e^3$ conveys a fast convergence rate. While the tracking positional error of $|e|$ is much smaller than 1, $g_3 \dot{e}^{[\beta]}$ conveys the role of defining finite time convergence.

According to the SMC principle, when the system's tracking positional error runs in sliding mode, the following equation should be satisfied ([9]):

$$s = 0 \text{ and } \dot{s} = 0 \tag{9}$$

Accordingly, from Eq. (7) and Eq. (9), it is obtained that

$$\ddot{e} + g_0 e^{[\gamma]} + g_1 e + g_2 e^3 + g_3 \dot{e}^{[\beta]} = 0 \tag{10}$$

Therefore, the following dynamic system of the sliding mode can be acquired as

$$\ddot{e} = -g_0 e^{[\gamma]} - g_1 e - g_2 e^3 - g_3 \dot{e}^{[\beta]} \tag{11}$$

Consequently, the following theorem is generated to complete the proof of convergence within a known finite time.

Theorem 1: For the following dynamic system of Eq. (11), the original points $e_i = 0, (i = 1, 2, \ldots, n)$ are globally balanced points in finite time.

Stability Analysis: Defines the following Lyapunov function candidate as

$$V_1 = \frac{g_0}{\gamma+1} |e|^{\gamma+1} + \frac{g_1}{2} e^2 + \frac{g_2}{4} e^4 + \frac{1}{2} \dot{e}^2 \tag{12}$$

With Eq. (11) the time derivative of Eq. (12) is derived as

$$\begin{aligned} \dot{V}_1 &= g_0 |e|^{[\gamma]} \dot{e} + g_1 e\dot{e} + g_2 e^3 \dot{e} + \dot{e}\ddot{e} \\ &= g_0 |e|^{[\gamma]} \dot{e} + g_1 e\dot{e} + g_2 e^3 \dot{e} \\ &\quad + \dot{e} \left(-g_0 e^{[\gamma]} - g_1 e - g_2 e^3 - g_3 \dot{e}^{[\beta]} \right) \\ &= -g_2 |\dot{e}|^{1+\beta} \leq 0 \end{aligned} \tag{13}$$

As a result, the condition for the Lyapunov stability principle is fulfilled. Next, the original point of the system in Eq. (11) is needed to prove a point as globally stable in finite time.

From the system in Eq. (11), this can be given as

$$\dot{e} = \psi(e) + \hat{\psi}(e) \tag{14}$$

with

$$\begin{aligned} \psi(e) &= \begin{pmatrix} \dot{e} \\ -g_0 e^{[\gamma]} - g_2 \dot{e}^{[\beta]} \end{pmatrix}, \\ \hat{\psi}(e) &= \begin{pmatrix} \hat{\psi}_1(e) \\ \hat{\psi}_2(e) \end{pmatrix} = \begin{pmatrix} 0 \\ -g_1 e - g_2 e^3 \end{pmatrix} \end{aligned} \tag{15}$$

when $\hat{\psi}(e) = 0$; the system in Eq. (14) becomes the form of the system under the feedback control law (54-55). It is a globally stable solution in finite time, according to Lemma 2 shown in the Appendix.

Accordingly, using Lemma 1, the original point of the dynamic system of Eq. (14) is a globally balanced point in case Eq. (53) that is satisfied with a disturbance vector $\hat{\psi}(e)$.

Based on Definition 2 shown in the Appendix, the system of $\dot{e} = \psi(e)$ is homogeneous of negative degree $p = \gamma - 1 < 0$ with respect to the dilation $(r_1, r_2) = (2, 1+\gamma)$. It is sure that $r_1 - r_2 - p > 0$. Hence,

$$\lim_{\lambda \to 0} \frac{\hat{\psi}_2(\lambda^{r_1} e, \lambda^{r_2} \dot{e})}{\lambda^{r_2+p}} = \lim_{\lambda \to 0} \frac{-g_1 \lambda^{r_1} e - g_2 \lambda^{3r_1} e^3}{\lambda^{r_2+p}} = 0, \quad \forall e \neq 0 \tag{16}$$

Accordingly, $\hat{\psi}(e) = 0$ satisfies the condition from Lemma 1 shown in the Appendix; hence, the original point of the dynamic system ($e = 0$) is a locally balanced point in finite time.

Proof of stability has been fulfilled.

Given the suitable NTSM surfaces have already been selected, the next task is designing a controller such that the sliding mode motion occurs in a finite time.

Remark 2: The NTSM surfaces proposed in Eq. (7) are totally different from the previously proclaimed surfaces referenced by TSM [13]–[15] and Fast TSM [19], [20]. Their sliding surfaces are expressed respectively in the form of the following equations:

$$\begin{aligned} s &= \dot{e} + \mu e^{q/l}, \\ s &= \dot{e} + \rho e + \mu e^{q/l}. \end{aligned} \tag{17}$$

in which ρ and μ are defined positive coefficients, and l, q are positive odd integers that satisfy the condition $1 < l/q < 2$. It can be clearly observed that, for $e < 0$, the fractional power l/q can cause the component of $e^{q/l} \notin \mathbb{R}$. Additionally, the control input in [19] encompasses $e^{\frac{q}{l}-1}\dot{e}$, which may cause a singularity in cases $\dot{e} \neq 0$ and $e = 0$.

To overcome obstacles of the complex-valued problem in Eq. (17), Yu *et al.* [22] suggested another form of TSM surface as

$$\begin{aligned} s &= \dot{e} + \mu |e|^{\gamma} sign(e), \\ s &= \dot{e} + \rho e + \mu |e|^{\gamma} sign(e). \end{aligned} \tag{18}$$

With the sliding surface of Eq. (18), the complex-valued number problem has been solved, but the control input has also encountered the singularity drawback in cases of $e_2 \neq 0$ and $e_1 = 0$.

In recent years, some new forms of NTSM surfaces were proposed to deal with the singularity obstacle [20]–[22]:

$$s = e + \frac{1}{\mu}\dot{e}^{l/q} \tag{19}$$

Nonetheless, the restriction of this sliding surface is that q and l must be positive odd integers. Accordingly, the proposed NTSM surface in this paper has not encountered the singularity drawback as discussed above.

B. DESIGN OF THE PROPOSED CONTROL ALGORITHM

As mentioned before, the appropriate finite time NTSM surface in the form of Eq. (7) has been selected, and the next task is to construct a control algorithm satisfying the control target in Section 2. Further, to obtain the desired performance for System (4) with Assumption 1, the following control law is presented in Theorem 2.

Theorem 2: For the dynamic system in state space as shown in Eq. (4), if the control input signal is constructed as (20-22), a suitable finite time NTSM surface is selected as shown in Eq. (7), and positive coefficients of Ψ satisfying Assumption 1 exist. This means that the system tracking position x_1 will reach the desired trajectory values x_d in a finite time. Accordingly, the goal of achieving global stability in a finite time is guaranteed.

The proposed controller based on the NTSM surface variable is designed as

$$u(t) = -Q(\mathrm{x}, t)^{+} \left(u_{eq}(t) + u_s(t)\right) \tag{20}$$

$$u_{eq}(t) = \left(H(\mathrm{x}, t) - \ddot{x}_d + g_0 e^{[\gamma]} + g_1 e + g_2 \dot{e}^{[\beta]} + \Upsilon s\right) \tag{21}$$

$$u_s(t) = (\Psi + \eta)\, sign(s) \tag{22}$$

where $Q^{+}(\mathrm{x}, t) = Q^{T}(\mathrm{x}, t)\left[Q(\mathrm{x}, t) Q^{T}(\mathrm{x}, t)\right]^{-1}$, and Υ, η, and Ψ are positive constants.

Stability Analysis: With System (4), $\ddot{e}$ is present as

$$\ddot{e} = \dot{x}_2 - \ddot{x}_d = H(\mathrm{x}, t) + D(\mathrm{x}, t) + Q(\mathrm{x}, t)\, u(t) - \ddot{x}_d \tag{23}$$

Inserting (23) into the time derivative of the NTSM variable of (7) gives

$$\begin{aligned} \dot{s} &= \ddot{e} + g_0 e^{[\gamma]} + g_1 e + g_2 e^3 + g_3 \dot{e}^{[\beta]} \\ &= H(\mathrm{x}, t) + D(\mathrm{x}, t) + Q(\mathrm{x}, t)\, u(t) \\ &\quad - \ddot{x}_d + g_0 e^{[\gamma]} + g_1 e + g_2 e^3 + g_3 \dot{e}^{[\beta]} \end{aligned} \tag{24}$$

Applying the control law (20-22) to (24) obtains

$$\begin{aligned} \dot{s} &= H(\mathrm{x}, t) + D(\mathrm{x}, t) + g_0 e^{[\gamma]} + g_1 e + g_2 e^3 + g_3 \dot{e}^{[\beta]} \\ &\quad + Q(\mathrm{x}, t)\left(-Q(\mathrm{x}, t)^{+}\left(u_{eq}(t) + u_s(t)\right)\right) - \ddot{x}_d \\ &= H(\mathrm{x}, t) + D(\mathrm{x}, t) - \ddot{x}_d + g_0 e^{[\gamma]} + g_1 e + g_2 e^3 + g_3 \dot{e}^{[\beta]} \\ &\quad - \left(\begin{pmatrix} H(\mathrm{x}, t) - \ddot{x}_d + g_0 e^{[\gamma]} + g_1 e \\ + g_2 e^3 + g_3 \dot{e}^{[\beta]} + \Upsilon s \end{pmatrix} + (\Psi + \eta)\, sign(s)\right) \\ &= -\Upsilon s + D(\mathrm{x}, t) - (\Psi + \eta)\, sign(s) \end{aligned} \tag{25}$$

Let us define the following Lyapunov function candidate as

$$V_2 = \frac{1}{2} s^T s \tag{26}$$

From (25), the time derivative of Eq. (26) is then derived as

$$\begin{aligned} \dot{V}_2 &= s^T \dot{s} = s^T \left(-\Upsilon s + D(\mathrm{x}, t) - (\Psi + \eta)\, sign(s)\right) \\ &= -\Upsilon s^T s + D(\mathrm{x}, t)\, s - \Psi s - \eta |s| \end{aligned} \tag{27}$$

Using Assumption 1, the following inequality is obtained as

$$\dot{V}_2 \leq -\Upsilon s^T s - \eta |s| \leq 0 \tag{28}$$

According to the Lyapunov stability criterion [34], [35], the stability and convergence of the error variables have been secured despite terrible conditions such as disturbances,

dynamic uncertainties, or faults. It also means positive coefficients of Ψ exist, which satisfying the condition of Eq. (5). Hence, Theorem 2 has been proved.

In comparison with Theorem 2 that is subject to the traditional SMC in terms of chattering behavior, the suggested system has significantly less chattering behavior in the control input. Both methods demand prior information regarding the upper bounds of the uncertainty terms; unfortunately, this prior information is not always accessible in real systems. In an unknown bound case, for (27) to be ensured, the design parameters selected in control law should be greater than the upper-bounds uncertainties. One weak point is that greater design parameters yield more serious chattering behavior. To overcome these control performance limitations, our method applies an adaptive technique to approximate the design parameters of the reaching control law and obtain the desired control algorithm.

Therefore, the proposed controller based on the NTSM surface variable and adaptive technique as depicted in Fig. 1 is designed as

$$u(t) = -Q(\mathrm{x}, t)^{+}\left(u_{eq}(t) + u_{as}(t)\right) \tag{29}$$

where $u_{eq}(t)$ is constructed the same as the equivalent control term in Eq. (21), and the adaptive control term is constructed as

$$u_{as}(t) = \left(\hat{\Psi}_{ad} + \eta\right) sign(s) \tag{30}$$

where $u_{eq}(t)$ is constructed identically to the equivalent control term in Eq. (21), and the adaptive control term is constructed as

$$\dot{\hat{\Psi}}_{ad} = \frac{1}{\kappa}|s| \tag{31}$$

where $\kappa > 0$ indicates the adaptive gain.

The following theorem is formulated for the proposed controller to achieve the control objective for the robotic system of Eq. (4).

Theorem 3: For the dynamic system in state space as Eq. (4), if the control input signal is constructed (29-30) with its parameter updating law as in Eq. (31) and a suitable finite time NTSM surface is selected as in Eq. (7), the estimating value of $\hat{\Psi}_{ad}$ has an upper limit. It means that there exists a positive coefficient of $\hat{\Psi}_{ad}$ satisfying the following condition:

$$\hat{\Psi}_{ad} \le \Psi^{*} \tag{32}$$

Furthermore, this means that the system tracking position x_1 will reach the desired trajectory values x_d in finite time. Accordingly, the goal of achieving global stability in finite time is guaranteed.

Stability Analysis: Proof of stability will be done according to the following approach.

Firstly, it will be shown there exist positive coefficients Ψ^{*} satisfying the condition of Eq. (32), which causes the system tracking position x_1 to reach the desired trajectory values x_d.

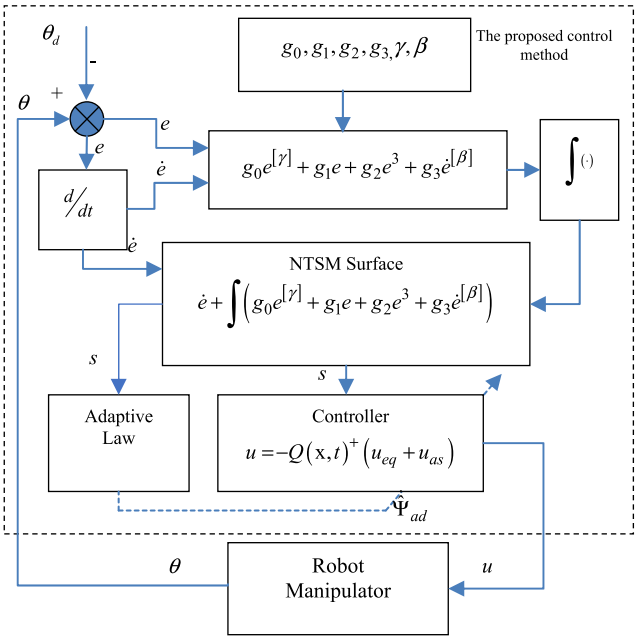

FIGURE 1. Block diagram of the proposed control method.

The following positive-definite Lyapunov functional is considered:

$$V_3 = \frac{1}{2}s^T s + \frac{1}{2}\kappa\left(\hat{\Psi}_{ad} - \Psi\right)^T\left(\hat{\Psi}_{ad} - \Psi\right) \tag{33}$$

where κ is a positive constant. Utilizing the same method employed to obtain (25), the time derivative of Eq. (33) is derived as

$$\begin{aligned}\dot{V}_3 &= s^T\dot{s} + \kappa\left(\hat{\Psi}_{ad} - \Psi\right)^T\dot{\hat{\Psi}}_{ad} \\ &= s^T\begin{pmatrix} -\Upsilon s + D(\mathrm{x}, t) \\ -\left(\hat{\Psi}_{ad} + \eta\right) sign(s)\end{pmatrix} + \kappa\left(\hat{\Psi}_{ad} - \Psi\right)\dot{\hat{\Psi}}_{ad}\end{aligned} \tag{34}$$

Inserting the adaptive rule (31) into (34) yields

$$\begin{aligned}\dot{V}_3 = -\Upsilon s^T s + D(\mathrm{x}, t)\, s - \hat{\Psi}_{ad}|s| \\ - \eta|s| + \left(\hat{\Psi}_{ad} - \Psi\right)|s|\end{aligned} \tag{35}$$

Applying Assumption 1, the following inequality is obtained as

$$\begin{aligned}\dot{V}_3 &= -\Upsilon s^T s + D(\mathrm{x}, t)\, s - \hat{\Psi}_{ad}|s| - \eta|s| \\ &\quad + \left(\hat{\Psi}_{ad} - \Psi\right)|s| \\ &= -\Upsilon s^T s + D(\mathrm{x}, t)\, s - \Psi|s| - \eta|s| \\ &\le -\Upsilon s^T s - \eta|s| \le -\eta|s| \le 0\end{aligned} \tag{36}$$

According to the Lyapunov stability criterion [34], [35], the estimating parameter of $\hat{\Psi}_{ad}$ is limited. It means that there exist positive coefficients of Ψ^{*} satisfying the condition of Eq. (32). Thus, Eq. (32) is proved.

Then, the method will continue to show that the system of Eq. (4) will attain the NTSM surfaces $s = 0$ in a finite time. We use the following proof procedure ([10]).

Consider the following Lyapunov function candidate as

$$V_4 = \frac{1}{2}s^T s + \frac{1}{2}v\tilde{\Psi}^T\tilde{\Psi} \tag{37}$$

where v is the positive coefficient, $\tilde{\Psi} = \hat{\Psi} - \Psi^*$.

The time derivative of Eq. (37) is derived as

$$\begin{aligned}\dot{V}_4 &= s^T\dot{s} + v\tilde{\Psi}^T\dot{\tilde{\Psi}} \\ &= s^T\left(-\Upsilon s + D(\mathrm{x},t) - \left(\hat{\Psi}_{ad} + \eta\right)sign(s)\right) \\ &\quad + v\left(\hat{\Psi}_{ad} - \Psi^*\right)\dot{\hat{\Psi}}_{ad}\end{aligned} \tag{38}$$

Inserting the adaptive rule (31) into (38) and using (32) yields

$$\begin{aligned}\dot{V}_4 &= s^T\left(-\Upsilon s + D(\mathrm{x},t) - \left(\hat{\Psi}_{ad} + \eta\right)sign(s)\right) \\ &\quad + v\left(\hat{\Psi}_{ad} - \Psi^*\right)\frac{1}{\kappa}|s| \\ &= -\Upsilon s^T s + D(\mathrm{x},t)\,s - \hat{\Psi}_{ad}|s| - \eta|s| + \frac{v}{\kappa}\left(\hat{\Psi}_{ad} - \Psi^*\right)|s| \\ &\le -\Upsilon s^T s + \Psi s - \hat{\Psi}_{ad}|s| - \eta|s| + \frac{v}{\kappa}\left(\hat{\Psi}_{ad} - \Psi^*\right)|s| \\ &\le \Psi s - \hat{\Psi}_{ad}|s| + \frac{v}{\kappa}\left(\hat{\Psi}_{ad} - \Psi^*\right)|s| + \Psi^*|s| - \Psi^*|s| \\ &= -\left(\Psi^* - \Psi\right)|s| + \frac{v}{\kappa}\left(\hat{\Psi}_{ad} - \Psi^*\right)|s| - \left(\hat{\Psi}_{ad} - \Psi^*\right)|s| \\ &= -\left(\Psi^* - \Psi\right)|s| - \left(-|s| + \frac{v}{\kappa}|s|\right)\left|\hat{\Psi}_{ad} - \Psi^*\right|\end{aligned} \tag{39}$$

For a simpler description, some symbols are defined as

$$\begin{cases}\Lambda_0 = (\Psi^* - \Psi) \\ \Lambda_1 = \left(-|s| + \frac{v}{\kappa}|s|\right)\end{cases} \tag{40}$$

Ψ^*, and v must be selected to satisfy the conditions that $\Psi^* > \Psi$ and $v > \kappa$. It follows that $\Lambda_0 > 0$ and $\Lambda_1 > 0$. Therefore, the following result is obtained:

$$\begin{aligned}\dot{V}_4 &\le -\Lambda_0|s| - \Lambda_1\left|\hat{\Psi}_{ad} - \Psi^*\right| \\ &\le -\sqrt{2}\Lambda_0\frac{|s|}{\sqrt{2}} - \Lambda_1\sqrt{\frac{2}{v}}\sqrt{v}\frac{\left|\hat{\Psi}_{ad} - \Psi^*\right|}{\sqrt{2}} \\ &\le -\min\left\{\sqrt{2}\Lambda_0, \Lambda_1\sqrt{\frac{2}{v}}\right\}\cdot\left(\frac{|s|}{\sqrt{2}} + \sqrt{v}\frac{\left|\hat{\Psi}_{ad} - \Psi^*\right|}{\sqrt{2}}\right)\end{aligned} \tag{41}$$

Using Jensen's inequality of Lemma 4 shown in the Appendix and defining that $\Lambda = \min\left\{\sqrt{2}\Lambda_0, \Lambda_1\sqrt{\frac{2}{v}}\right\}$, the following results are consequently obtained:

$$\begin{aligned}\dot{V}_4 &\le -\Lambda\left(\frac{s^T s}{\left(\sqrt{2}\right)^2} + \left(\sqrt{v}\right)^2\frac{\left(\hat{\Psi}_{ad} - \Psi^*\right)^T\left(\hat{\Psi}_{ad} - \Psi^*\right)}{\left(\sqrt{2}\right)^2}\right)^{\frac{1}{2}} \\ &\le -\Lambda V_4^{1/2}\end{aligned} \tag{42}$$

Based on Lemma 3 shown in the Appendix, it is shown that the controlled variables in Eq. (4) reach the NTSM variable

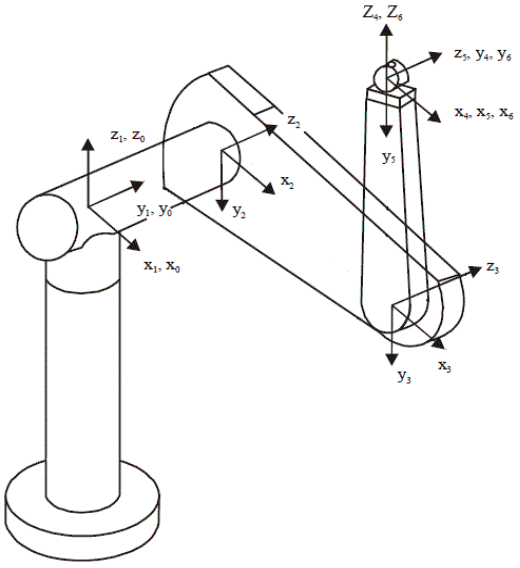

FIGURE 2. 3−DOF PUMA560 robot manipulator.

in a known amount of time $T \le \frac{2V_4^{1/2}(0)}{\Lambda}$. Furthermore, once the NTSM surface converges to zero, then the tracking error of the robot system will also become zero. This completes the proof of Theorem 3.

Remark 3: In real systems, the parameter drift matter usually occurs under adaptive law (31). Therefore, the bounded method is performed to set up the adaptive law as

$$\dot{\hat{\Psi}}_{ad} = \begin{cases}0 & \text{if } |s| \le \upsilon \\ \frac{1}{\kappa}|s| & \text{if } |s| > \upsilon\end{cases} \tag{43}$$

in which $\upsilon > 0$ is an arbitrary positive value.

Theoretically, the proposed control algorithm contains the discontinuous term $\left(\hat{\Psi}_{ad} + \eta\right)sign(s)$ that may cause chattering phenomenon from an infinite switching frequency of a discontinuous term. To reject the possible chattering phenomenon, some procedures have been used. For example, the function of $s/(|s| + \varepsilon^*)$ can be utilized to approximate the function of $sign(s)$ (in which ε^* is a minor positive coefficient) or another technique is applied in this paper, which is summarized in Remark 4.

Remark 4 [22]: The chattering phenomenon can be significantly alleviated by replacing the $sign(\cdot)$ function with a saturation function in the control input signal, such as

$$\mathrm{sat}\left(\frac{s}{\varepsilon^*}\right) = \begin{cases}sign(s) & \text{if } |s| \ge \varepsilon^* \\ \frac{s}{\varepsilon^*} & \text{if } |s| < \varepsilon^*\end{cases} \tag{44}$$

in which ε^* is a minor positive coefficient.

IV. NUMERICAL SIMULATION RESULTS

We consider a 3-DOF PUMA560 robot [36] with the first three joints and the last three joints blocked. Its kinematic illustration is shown in Fig. 2.

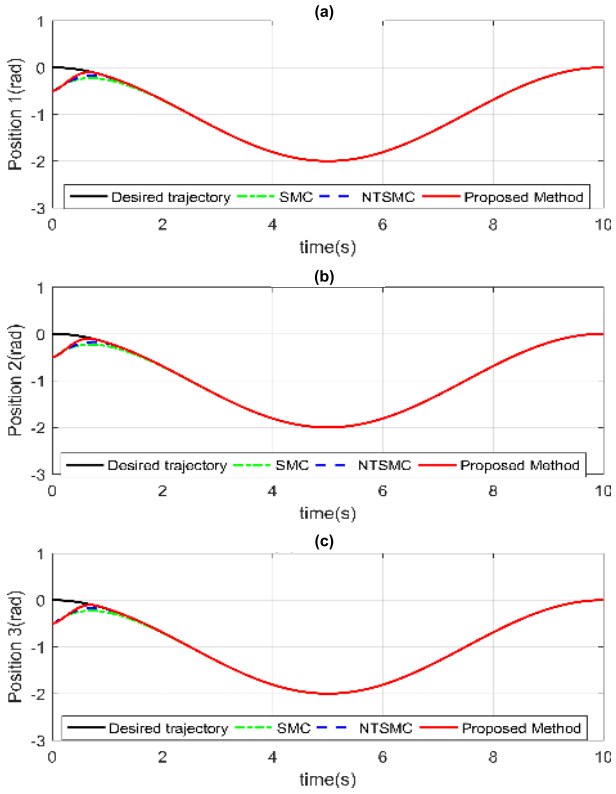

FIGURE 3. Tracking Positions with a sign function: (a) at Joint 1, (b) at Joint 2, and (c) at Joint 3.

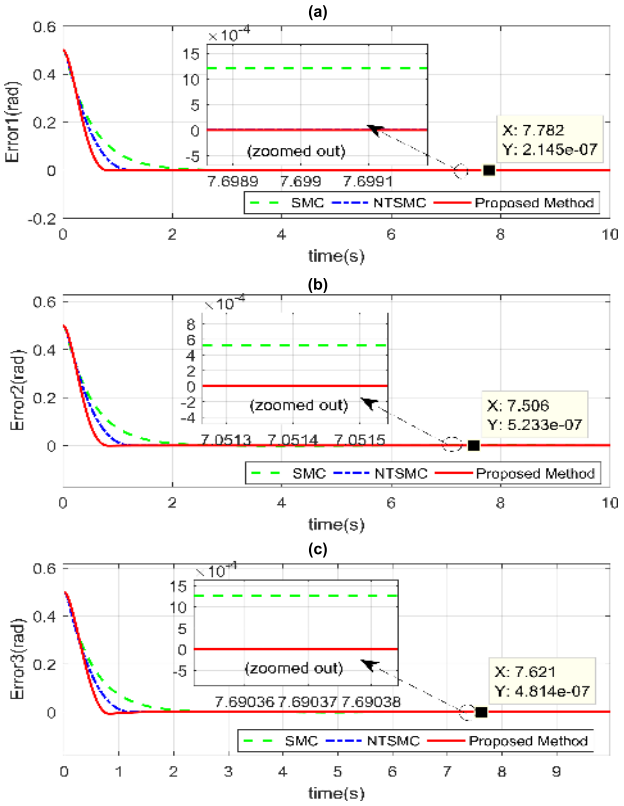

FIGURE 4. Tracking Errors with a sign function: (a) at Joint 1, (b) at Joint 2, and (c) at Joint 3.

The uncertainties in this simulation are assumed as follows. The friction $F_r\left(\dot{\theta}\right)$ and disturbance τ_D are assumed to be

$$F_r\left(\dot{\theta}\right)+\tau_D=\begin{bmatrix} 2.1\dot{\theta}_1+2.02sign\left(3\dot{\theta}_1\right) \\ 4.2\dot{\theta}_2+2.2sign\left(2\dot{\theta}_2\right) \\ 1.1\dot{\theta}_3+1.15sign\left(2\dot{\theta}_3\right) \end{bmatrix}+\begin{bmatrix} 7.2sin\left(\dot{\theta}_1\right) \\ 6.1sin\left(\dot{\theta}_2\right) \\ 4.15sin\left(\dot{\theta}_3\right) \end{bmatrix} \tag{45}$$

The desired joint trajectories are

$$\theta_d=\left[\cos\left(\tfrac{t}{5\pi}\right)-1\ \sin\left(\tfrac{t}{5\pi}+\tfrac{\pi}{2}\right)-1\ \sin\left(\tfrac{t}{5\pi}+\tfrac{\pi}{2}\right)-1\right]^T \tag{46}$$

The parameters for the NTSM surface in Eq. (7) and the controlling input (29-31) are experimentally selected as $g_0=15, g_1=6, g_2=3, g_3=10, \gamma=0.2, \beta=0.6, \Upsilon=20, \kappa=0.1, \varepsilon^*=0.15$, and $\eta=0.2$. The initial values of the system are chosen as $\theta_1(0)=-0.5$, $\theta_2(0)=-0.5$, and $\theta_3(0)=-0.5$. The initial value of adaptive control law is selected as $\hat{\Psi}_{ad}(0)=0$.

To show the effectiveness of the proposed control algorithm, its trajectory tracking performances are compared with those of the conventional SMC [9]–[12] and the NTSM controller [20]–[22]. These control methods for comparison are briefly explained as follows.

The conventional SMC [11] has the control input

$$u(t)=-Q(\mathrm{x},t)^{-1}\begin{bmatrix} H(\mathrm{x},t)+\varphi(x_2-\dot{x}_d) \\ -\ddot{x}_d+(\Psi+\eta)\,sign(s) \end{bmatrix} \tag{47}$$

in which $s=\dot{e}+ce$ is the linear sliding surface.

The parameters of the controller in Eq. (47) were selected as $\Psi=19.8, \eta=0.2, c=2$ and $\varphi=2$ to obtain good simulation results.

Further, the NTSM controller [21] has the control input

$$u(t)=-Q(\mathrm{x},t)^{-1}\begin{bmatrix} H(\mathrm{x},t)+\mu\frac{q}{l}\dot{e}^{2-l/q} \\ -\ddot{x}_d+(\Psi+\eta)\,sign(s) \end{bmatrix} \tag{48}$$

in which $s=e+\mu^{-1}\dot{e}^{l/q}$ is a nonlinear sliding surface.

The parameters of the controller in Eq. (48) were selected as $q=3, l=5, \eta=0.2, \Psi=19.8$, and $\mu=2.0$ to obtain good simulation results.

The simulations were carried out in the following two cases to compare the controllers in terms of both positional accuracy and the resulting chattering behaviors in their control inputs.

Case 1: Each of three controllers has the discontinuous term of $sign(s)$ in its control input signal.

Case 2: Each of three controllers applied Remark 4 in which the discontinuous term of $sign(s)$ is replaced with a saturation function in its control input signal.

In Case 1, the tracking positions and tracking errors of the three joints with three control methods are given

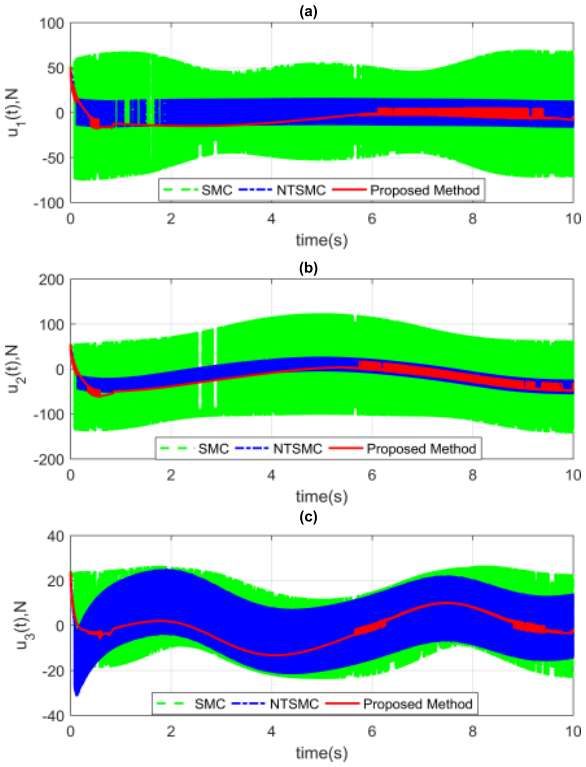

FIGURE 5. Control inputs with a sign function: (a) at Joint 1, (b) at Joint 2, and (c) at Joint 3.

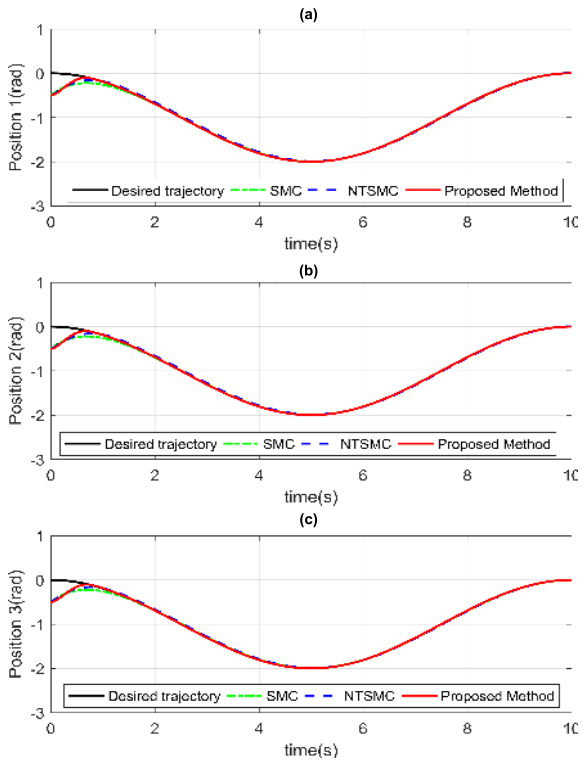

FIGURE 6. Tracking positions with a saturation function: (a) at Joint 1, (b) at Joint 2, and (c) at Joint 3.

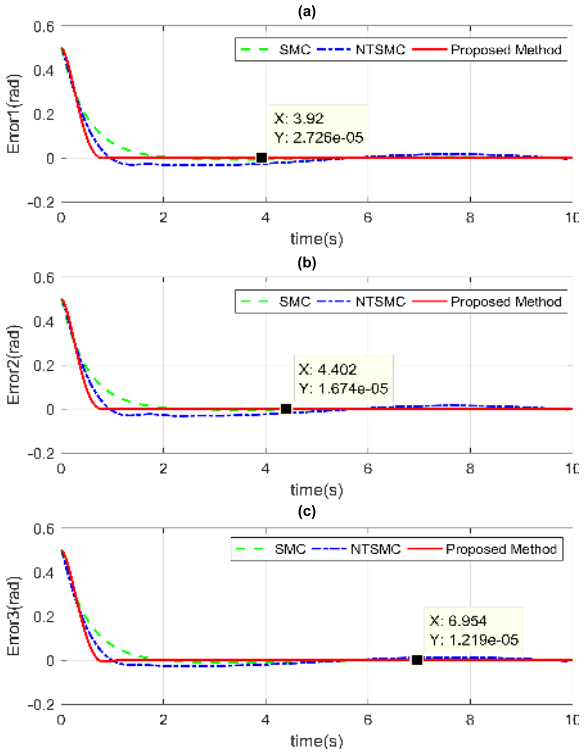

FIGURE 7. Tracking errors with a saturation function: (a) at Joint 1, (b) at Joint 2, and (c) at Joint 3.

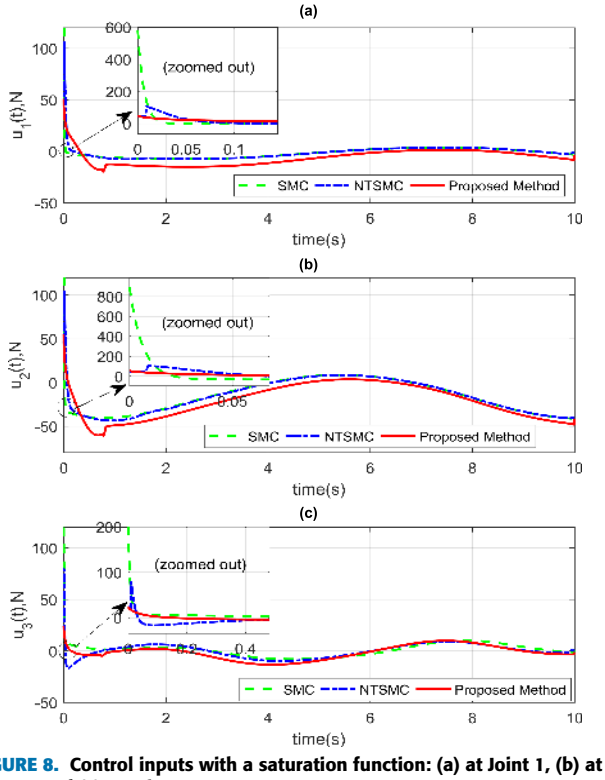

FIGURE 8. Control inputs with a saturation function: (a) at Joint 1, (b) at Joint 2, and (c) at Joint 3.

in Fig. 3 and Fig. 4, respectively. All three controllers offer similar good trajectory tracking performances. However, the tracking errors of the proposed controller are smaller than those of the other control methods by the order of 10^{-6} rad. The tracking errors of the other control methods are on the order of $10^{-4} \sim 10^{-5}$ rad. The more interesting finding involves comparison of the control inputs in terms of

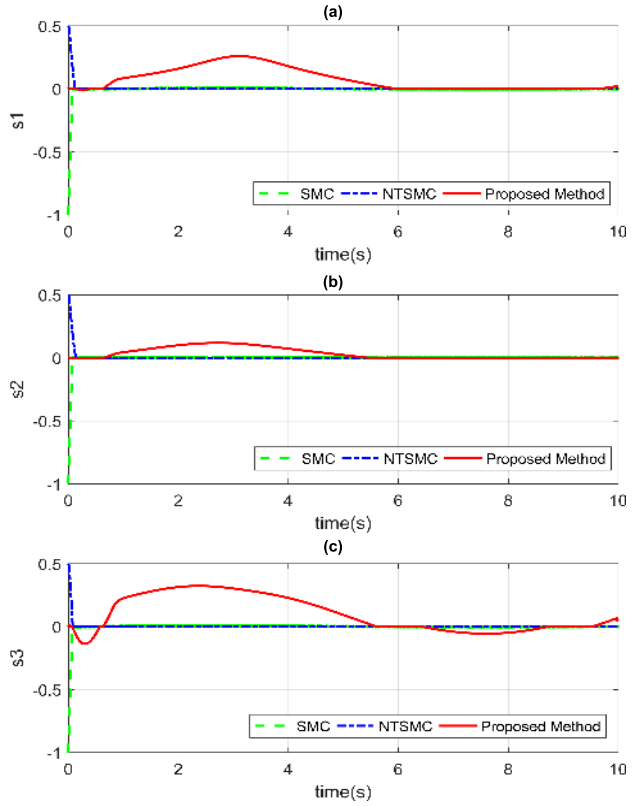

FIGURE 9. Non-singular terminal sliding surfaces with a sign function: (a) at Joint 1, (b) at Joint 2, and (c) at Joint 3.

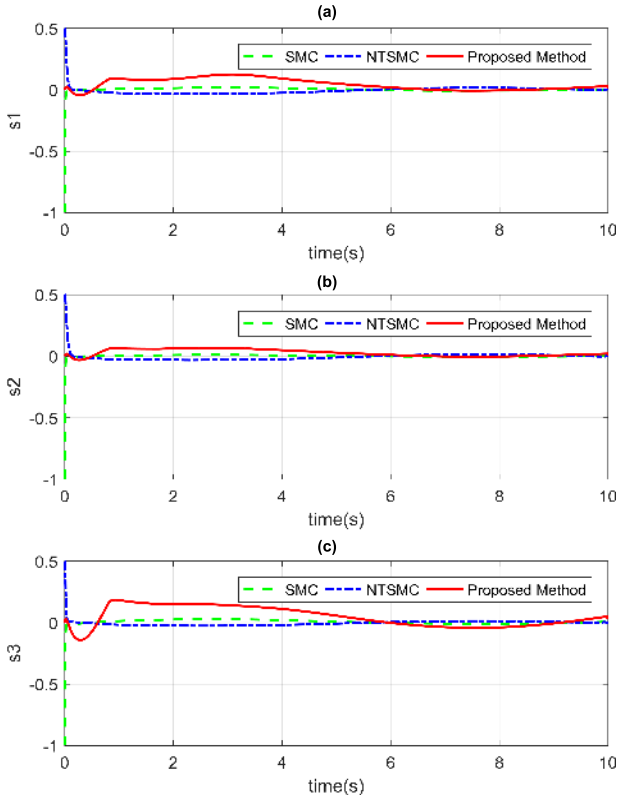

FIGURE 10. Non-singular terminal sliding surfaces with a saturation function: (a) at Joint 1, (b) at Joint 2, and (c) at Joint 3.

the chattering phenomena, shown in Fig. 5. The chattering behavior from the proposed NTSM surface and control law was shown as significantly less than those of the other control methods.

To reduce chattering, the saturation function has been adopted in SMC methods instead of the sign function. In this case, it is easily expected that reducing chattering often reduces positional accuracy. The simulation results of Case 2 confirm the expectant results shown in Figs. 6-8. Noteworthy is that the degradation of the tracking positional accuracies of the proposed control method is the smallest among the three controllers, while the chattering of the control inputs is in the allowable range. The tracking errors of the proposed controller are on the order of 10^{-6} rad, while those of the other control methods are worse, on the order of 10^{-3} rad. Furthermore, the required initial control input of the proposed control method seems to be an affordable magnitude, while those of the other control method seems to be too high and lead to motor torque saturation as shown in Fig. 8.

The response time of the sliding surface in two cases is shown in Figs. 9-10. It is shown that the proposed NTSM surface allows a faster finite time convergence trajectory than the old-style SMC and conventional NTSM surfaces. The transient response of the proposed NTSM surface has been improved and quickly responded to the

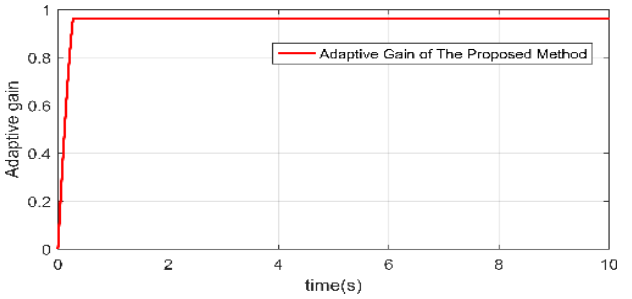

FIGURE 11. The response time of the estimating parameters with a sign function: (a) at Joint 1, (b) at Joint 2, and (c) at Joint 3.

fast variation of influences of the external disturbances or uncertainties.

The variations of the estimated parameter of $\hat{\Psi}_{ad}$ in two Case are shown in Figs. 11-12. The parameters are estimated according to the variation of the undefined parameters, and this estimated parameter will reach a constant when the system state variables converge to the non-singular sliding surfaces.

From the simulation results, it can be concluded that the proposed controller shows the best performance among the three in terms of tracking positional accuracy, small steady state error, fast response speed, and weak chattering behavior.

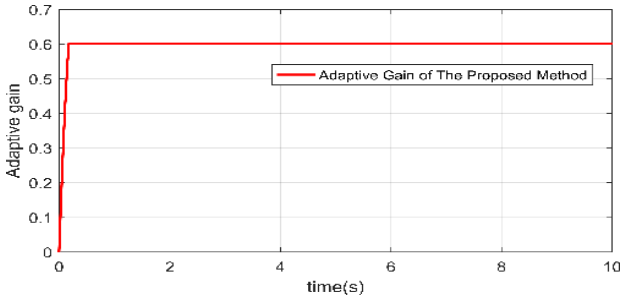

FIGURE 12. The response time of the estimating parameters with a saturation function: (a) at Joint 1, (b) at Joint 2, and (c) at Joint 3.

Remark 5: The robustness issue and the finite-time convergence of the suggested system are totally confirmed by the Lyapunov stability principle. Through simulation studies and comparison among those of the conventional SMC [9]–[12] and the NTSM controller [20]–[22], the experimental results and performance comparison could be expected to show the effectiveness and viability of our proposed scheme for the joint position tracking control of a 3-DOF PUMA560 robot. In the next work, authors will apply the proposed controller to the real robot system and compare with other state-of-the-art controllers to demonstrate the effectiveness of this control method.

V. CONCLUSION

In this paper, an adaptive continuous finite time terminal sliding mode control (TSMC) algorithm is presented for robot manipulators. From the simulation and performance comparison with two other control methods for a 3-DOF PUMA560 robot, the suggested control method shows the best performance among the three controllers in terms of tracking positional accuracy, small steady state error, fast response speed, and weak chattering behavior. We think that the proposed control algorithm has the following important characteristics: 1) the NTSM surface allows finite time convergence without singularity, 2) requires no prior information of the upper limits of uncertainties, 3) shows tremendously less chattering behavior, and 4) the magnitude of the generated control input seems to be more suitable in terms of motor torque saturation compared with those of the other control methods.

APPENDIX

Some preliminary definitions applied in the progress of the control scheme are introduced in this part.

Consider the following system

$$\dot{x} = \psi(x), \quad \psi(x) = 0 \tag{49}$$

where $x \in \Omega \subset \mathbb{R}^n, x(0) = x_0$

Definition 1 [37]: The original point is termed a globally balanced point of the system (49) in finite time in the case of an open neighborhood $\mathbb{N} \subseteq \Omega$ of the original point and a function $T : \mathbb{N}\backslash\{0\} \to (0, \backslash\infty)$, termed the settling time, such that the following criterion holds:

Finite time convergence property: For every $x_0 \in \mathbb{N}\backslash\{0\}$, every solution $x(t, x_0)$ is defined for $t \in [0, T(x_0)), x(t, x_0) \in \mathbb{N}\backslash\{0\}$, for $t \in [0, T(x_0))$ and, $\lim_{t \to T(x_0)} x(t, x_0) = 0$.

The Lyapunov stability criterion: For every open set $\mathcal{U}_s$ such that $0 \in \mathcal{U}_s \subseteq \mathbb{N}$, there exists an open set $\mathcal{U}_\delta$ such that $0 \in \mathcal{U}_s \subseteq \mathbb{N}$ and such that, for every $x_0 \in \mathcal{U}_\delta \backslash \{0\}, x(t, x_0) \in \mathcal{U}_s$ for all $t \in [0, T(x_0))$.

The original point is defined as a globally balanced point in finite time in the case that it is a finite-time balanced point and $\Omega = \mathbb{N} = \mathbb{R}^n$.

Definition 2: A family of dilations C_ε^r is a mapping that designates to every real $\lambda > 0$ a diffeomorphism

$$C_\lambda^r(x_1, x_2, \ldots, x_n) = (\lambda^{r_1} x_1, \lambda^{r_2} x_2, \ldots, \lambda^{r_n} x_n) \tag{50}$$

where $x_1, x_2, \ldots, x_n$ are appropriate coordinates on $\mathbb{R}^n$, and $r = r_1, r_2, \ldots, r_n$ with the dilation coefficients $r = r_1, r_2, \ldots, r_n$ are positive real numbers.

A vector field $\psi(x) = [\psi_1(x), \psi_2(x), \ldots, \psi_n(x)]^T$ is homogeneous to the degree $p \in \mathbb{R}$ with respect to the family of dilations for all $\lambda > 0$

$$\psi_l\left(\lambda^{r_1} x_1, \lambda^{r_2} x_2, \ldots, \lambda^{r_n} x_n\right) = \lambda^{p+r_l} \psi_l(x), \quad l = 1, 2, \ldots, n \tag{51}$$

The system of Eq. (49) is named homogeneous in the case its vector field ψ is homogeneous.

Lemma 1 [38]: The following non-linear system is considered:

$$\dot{x} = \psi(x) + \hat{\psi}(x), \quad x \in \mathbb{R}^n \tag{52}$$

where $\psi(x)$ is an n-dimensional continuous homogeneous vector field of degree $p < 0$ with dilation $(r_1, r_2, \ldots, r_n)$ satisfying $\psi(0) = 0$, and $\hat{\psi}$ is a continuous vector field satisfying $\hat{\psi}(0) = 0$. Assume $x = 0$ as an asymptotic balanced point of the system $\dot{x} = \psi(x)$. Then, the zero solution of Eq. (52) is a locally finite time stable result if

$$\lim_{\lambda \to 0} \left(\hat{\psi}_l\left(\lambda^{r_1} x_1, \lambda^{r_2} x_2, \ldots, \lambda^{r_n} x_n\right)\right) / \lambda^{p+r_l} = 0$$
$$l = 1, 2, \ldots, n, \forall x \neq 0 \tag{53}$$

Lemma 2 [38], [39]: The following system is considered

$$\begin{cases} \dot{x}_1 = x_2 \\ x_2 = u \end{cases} \tag{54}$$

The original point of the system of Eq. (54) is a globally balanced point in finite time according to the principle of feedback control:

$$u = -\mu_1 |x_1|^{\vartheta_1} sign(x_1) - \mu_2 |x_2|^{\vartheta_2} sign(x_2) \tag{55}$$

in which ϑ_1, ϑ_2 are positive coefficients, and $\vartheta_1, \ldots, \vartheta_n$ satisfy $\vartheta_{i-1} = \frac{\vartheta_i \vartheta_{i+1}}{2\vartheta_{i+1} - \vartheta_i}, i = 2, \ldots, n$, with $\vartheta_{i+1} = 1$ and $\vartheta_i = \vartheta$.

Lemma 3 [40]: Suppose that a continuous positive-definite function $\Delta(t)$ satisfies the differential inequality:

$$\dot{\Delta}(t) \leq -\alpha \Delta^\delta(t), \quad \forall t \geq t_0, \ \Delta(t_0) \geq 0 \tag{56}$$

in which $\delta > 0, 0 < \delta < 1$ are coefficients. Then, for any given t_0, $\Delta(t)$, the following inequality is satisfied:

$$\Delta^{1-\delta}(t) \leq \Delta^{1-\delta}(t_0) - \alpha(1-\delta)(t-t_0), \quad t_0 \leq t \leq t_1 \tag{57}$$

with $\Delta(t) = 0, \forall t \geq t_1$,
where t_1 is calculated by

$$t_1 = t_0 + \frac{1}{\alpha(1-\delta)}\Delta^{1-\delta}(t_0) \tag{58}$$

Lemma 4 ([41], Jensen's Inequality): It has the following form

$$\left(\sum_{i=1}^{m}\phi_i^{a_2}\right)^{1/a_2} \leq \left(\sum_{i=1}^{m}\phi_i^{a_1}\right)^{1/a_1}, \quad 0 < a_1 < a_2 \tag{59}$$

with $\phi_i \geq 0, 1 \leq i \leq m$.

REFERENCES

[1] S. Arimoto, "Stability and robustness of PID feedback control for robot manipulators of sensory capability," in *Proc. 1st Int. Symp. Robot. Res.*, 1984, pp. 783–799.

[2] M. W. Spong and M. Vidyasagar, *Robot Dynamics and Control*. New York, NY, USA: Wiley, 1989.

[3] J.-J. E. Slotine and W. Li, *Applied Nonlinear Control*, vol. 199. Upper Saddle River, NJ, USA: Prentice-Hall, 1991, no. 1.

[4] K. Lim and M. Eslami, "Robust adaptive controller designs for robot manipulator systems," *IEEE J. Robot. Autom.*, vol. JRA-3, no. 1, pp. 54–66, Feb. 1987.

[5] Y. Guo and P.-Y. Woo, "An adaptive fuzzy sliding mode controller for robotic manipulators," *IEEE Trans. Syst., Man, Cybern. A, Syst. Humans*, vol. 33, no. 2, pp. 149–159, Mar. 2003.

[6] A. T. Vo, H.-J. Kang, and V.-C. Nguyen, "An output feedback tracking control based on neural sliding mode and high order sliding mode observer," in *Proc. 10th Int. Conf. Hum. Syst. Interact. (HSI)*, Jul. 2017, pp. 161–165.

[7] F. Lin and R. D. Brandt, "An optimal control approach to robust control of robot manipulators," *IEEE Trans. Robot. Autom.*, vol. 14, no. 1, pp. 69–77, Feb. 1998.

[8] T. C. Hsia and S. Jung, "A simple alternative to neural network control scheme for robot manipulators," *IEEE Trans. Ind. Electron.*, vol. 42, no. 4, pp. 414–416, Aug. 1995.

[9] V. I. Utkin, *Sliding Modes in Control and Optimization*. Berlin, Germany: Springer-Verlag, 2013.

[10] F. Plestan, Y. Shtessel, V. Brégeault, and A. Poznyak, "New methodologies for adaptive sliding mode control," *Int. J. Control*, vol. 83, no. 9, pp. 1907–1919, 2010.

[11] C. Edwards and S. Spurgeon, *Sliding Mode Control: Theory and Applications*. Boca Raton, FL, USA: CRC Press, 1998.

[12] A. Levant, "Higher-order sliding modes, differentiation and output-feedback control," *Int. J. Control*, vol. 76, nos. 9–10, pp. 924–941, Jan. 2003.

[13] S. T. Venkataraman and S. Gulati, "Control of nonlinear systems using terminal sliding modes," *J. Dyn. Syst., Meas., Control*, vol. 115, no. 3, pp. 554–560, 1993.

[14] M. Zhihong, A. P. Paplinski, and H. R. Wu, "A robust MIMO terminal sliding mode control scheme for rigid robotic manipulators," *IEEE Trans. Autom. Control*, vol. 39, no. 12, pp. 2464–2469, Dec. 1994.

[15] Y. Wu, X. Yu, and Z. Man, "Terminal sliding mode control design for uncertain dynamic systems," *Syst. Control Lett.*, vol. 34, no. 5, pp. 281–287, 1998.

[16] X.-T. Tran and H.-J. Kang, "T-S fuzzy model-based robust finite time control for uncertain nonlinear systems," *Proc. Inst. Mech. Eng., C, J. Mech. Eng. Sci.*, vol. 229, no. 12, pp. 2174–2186, 2015.

[17] Y. Feng, J. Zheng, X. Yu, and N. V. Truong, "Hybrid terminal sliding-mode observer design method for a permanent-magnet synchronous motor control system," *IEEE Trans. Ind. Electron.*, vol. 56, no. 9, pp. 3424–3431, Sep. 2009.

[18] C. P. Tan, X. Yu, and Z. Man, "Terminal sliding mode observers for a class of nonlinear systems," *Automatica*, vol. 46, no. 8, pp. 1401–1404, 2010.

[19] X. Yu and Z. Man, "Fast terminal sliding-mode control design for nonlinear dynamical systems," *IEEE Trans. Circuits Syst.*, vol. 49, no. 2, pp. 261–264, Feb. 2002.

[20] L. Yang and J. Yang, "Nonsingular fast terminal sliding-mode control for nonlinear dynamical systems," *Int. J. Robust Nonlinear Control*, vol. 21, no. 16, pp. 1865–1879, Nov. 2011.

[21] Y. Feng, X. Yu, and Z. Man, "Non-singular terminal sliding mode control of rigid manipulators," *Automatica*, vol. 38, no. 12, pp. 2159–2167, 2002.

[22] S. Yu, X. Yu, B. Shirinzadeh, and Z. Man, "Continuous finite-time control for robotic manipulators with terminal sliding mode," *Automatica*, vol. 41, no. 11, pp. 1957–1964, Nov. 2005.

[23] M. Zhihong, M. O'Day, and X. Yu, "A robust adaptive terminal sliding mode control for rigid robotic manipulators," *J. Intell. Robot. Syst.*, vol. 24, no. 1, pp. 23–41, 1999.

[24] B. Mezghani, N. Romdhane, and T. Damak, "Adaptive terminal sliding mode control for rigid robotic manipulators," *Int. J. Autom. Comput.*, vol. 8, no. 2, pp. 215–220, 2011.

[25] L. Wang, T. Chai, and L. Zhai, "Neural-network-based terminal sliding-mode control of robotic manipulators including actuator dynamics," *IEEE Trans. Ind. Electron.*, vol. 56, no. 9, pp. 3296–3304, Sep. 2009.

[26] L. Qiao and W. Zhang, "Adaptive non-singular integral terminal sliding mode tracking control for autonomous underwater vehicles," *IET Control Theory Appl.*, vol. 11, no. 8, pp. 1293–1306, 2017.

[27] L. Qiao and W. Zhang, "Adaptive second-order fast nonsingular terminal sliding mode tracking control for fully actuated autonomous underwater vehicles," *IEEE J. Ocean. Eng.*, to be published.

[28] L. Qiao and W. Zhang, "Double-loop integral terminal sliding mode tracking control for UUVs with adaptive dynamic compensation of uncertainties and disturbances," *IEEE J. Ocean. Eng.*, to be published.

[29] R. R. Nair and L. Behera, "Robust adaptive gain nonsingular fast terminal sliding mode control for spacecraft formation flying," in *Proc. IEEE 54th Annu. Conf. Decis. Control (CDC)*, Dec. 2015, pp. 5314–5319.

[30] R. R. Nair, H. Karki, A. Shukla, L. Behera, and M. Jamshidi, "Fault-tolerant formation control of nonholonomic robots using fast adaptive gain nonsingular terminal sliding mode control," *IEEE Syst. J.*, to be published.

[31] J. Sun, Y. Shen, X. Wang, and J. Chen, "Finite-time combination-combination synchronization of four different chaotic systems with unknown parameters via sliding mode control," *Nonlinear Dyn.*, vol. 76, no. 1, pp. 383–397, 2014.

[32] M. P. Aghababa and H. P. Aghababa, "Adaptive finite-time synchronization of non-autonomous chaotic systems with uncertainty," *J. Comput. Nonlinear Dyn.*, vol. 8, no. 3, p. 031006, 2013.

[33] M. P. Aghababa and H. P. Aghababa, "A general nonlinear adaptive control scheme for finite-time synchronization of chaotic systems with uncertain parameters and nonlinear inputs," *Nonlinear Dyn.*, vol. 69, no. 4, pp. 1903–1914, 2012.

[34] A. Polyakov and L. Fridman, "Stability notions and Lyapunov functions for sliding mode control systems," *J. Franklin Inst.*, vol. 351, no. 4, pp. 1831–1865, 2014.

[35] Y. Hong, J. Huang, and Y. Xu, "On an output feedback finite-time stabilization problem," *IEEE Trans. Autom. Control*, vol. 46, no. 2, pp. 305–309, Feb. 2001.

[36] B. Armstrong, O. Khatib, and J. Burdick, "The explicit dynamic model and inertial parameters of the PUMA 560 arm," in *Proc. IEEE Int. Conf. Robot. Automat.*, vol. 3, Apr. 1986, pp. 510–518.

[37] S. P. Bhat and D. S. Bernstein, "Continuous finite-time stabilization of the translational and rotational double integrators," *IEEE Trans. Autom. Control*, vol. 43, no. 5, pp. 678–682, May 1998.

[38] S. P. Bhat and D. S. Bernstein, "Geometric homogeneity with applications to finite-time stability," *Math. Control, Signals, Syst.*, vol. 17, no. 2, pp. 101–127, Jun. 2005.

[39] X.-T. Tran and H.-J. Kang, "A novel adaptive finite-time control method for a class of uncertain nonlinear systems," *Int. J. Precis. Eng. Manuf.*, vol. 16, no. 13, pp. 2647–2654, 2015.

[40] Y. Tang, "Terminal sliding mode control for rigid robots," *Automatica*, vol. 34, no. 1, pp. 51–56, 1998.

[41] E. M. Fels, "Beckenbach, E. F., and Bellman R.: Inequalities, Springer Verlag, Berlin-Göt-tingen-Heidelberg, 1961. ([Hungarian Language Ignored]) 276 Seiten, Preis 1 r. 9 k," *Biometrical J.*, vol. 8, no. 4, p. 279, 1966.

ANH TUAN VO received the B.S. degree in electrical engineering from the Da Nang University of Technology, Da Nang, Vietnam, in 2008. He is currently pursuing the Ph.D. degree with the School of Electrical Engineering, University of Ulsan, Ulsan, South Korea. His research interests include intelligent control, sliding mode control, robot fault diagnosis, and fault tolerant control.

HEE-JUN KANG received the B.S. degree from Seoul National University, South Korea, in 1985, and the M.S. and Ph.D. degrees from The University of Texas at Austin, USA, in 1988 and 1991, respectively, all in mechanical engineering. Since 1992, he has been a Professor of electrical engineering with the University of Ulsan. His current research interests include sensor-based robotic application, robot calibration, haptics, robot fault diagnosis, and mechanism analysis.